Available online at www.sciencedirect.com
ScienceDirect
International Journal of Heat and Fluid Flow 28 (2007) 1272–1279
International Journal of HEAT AND FLUID FLOW
www.elsevier.com/locate/ijhff

Instantaneous fluctuation velocity and skewness distributions upstream of transition onset

D. Hernon [a,*], E.J. Walsh [a], D.M. McEligot [b,c,d]

[a] Stokes Research Institute, Department of Mechanical and Aeronautical Engineering, University of Limerick, Ireland
[b] Idaho National Laboratory (INL), Idaho Falls, ID 83415-3885, USA
[c] University of Arizona, AZ 85721, USA
[d] University of Stuttgart, D-70550 Stuttgart, Germany

Received 5 December 2006; received in revised form 9 May 2007; accepted 11 May 2007
Available online 6 July 2007

Abstract

The development of streamwise orientated disturbances through the boundary layer thickness prior to transition onset for zero-pressure gradient boundary layer flow under the influence $\%Tu = 4.2$ is presented. The analysis concentrates on the development of the maximum positive and negative of the fluctuation velocity in order to gain further insight into the transition process. The average location of the peak negative fluctuation velocity over a range of Reynolds numbers was measured in the upper portion of the boundary layer at $y/\delta \approx 0.6$, whereas the location of the peak positive value was measured at $y/\delta \approx 0.3$. The disturbance magnitude of the negative fluctuation velocity increased beyond that of the positive as transition onset approached. The distribution and disturbance magnitude of the maximum positive and negative fluctuation velocities indicate that the initiation of transition may occur on the low-speed components of the flow that are lifted up to the upper region of the boundary layer. This is in qualitative agreement with recent direct numerical simulations on the breakdown of the flow on the lifted low-speed streaks near the boundary layer edge. The results presented in this investigation also demonstrate the increased physical insight gained by examining the distributions of the maximum positive and negative of the streamwise fluctuation velocity component associated with the low- and high-speed streaks, compared to time-averaged values, in determining what structures cause the breakdown to turbulence.
© 2007 Elsevier Inc. All rights reserved.

Keywords: Transition; Streaky structures; Pre-transitional flow; Boundary layer instability

1. Introduction

Under elevated freestream turbulence (FST) conditions, usually greater than 1%Tu (where Tu is the turbulence intensity at the leading edge), the mode of transition is termed bypass. Recent direct numerical simulation (DNS) investigations by Jacobs and Durbin (2001), Brandt et al. (2004) and Zaki and Durbin (2005) have further elucidated some of the mechanisms of bypass transition. The DNS results of Jacobs and Durbin (2001) illustrated that turbulent spots are formed when a backward jet, which is a component of a low-speed laminar streak, lifts off the surface to the upper portion of the laminar boundary layer. There it may couple to high-frequency disturbances from the freestream and the ensuing instability grows until the creation of a turbulent spot. Brandt et al. (2004) demonstrated the initial stages of the bypass transition process to contain elongated streaky structures of both positive and negative fluctuation velocity (u) which can develop a streamwise waviness and breakdown into turbulent spots via varicose or sinuous secondary instabilities. Brandt et al. (2004) also examined the receptivity of the boundary layer by varying the energy spectrum of the incoming perturbation. They demonstrated that the transition location moved to lower

* Corresponding author. Present address: Bell Labs Ireland, Blanchardstown Industrial Estate, Dublin 15, Ireland.
E-mail address: hernon@alcatel-lucent.com (D. Hernon).

0142-727X/$ - see front matter © 2007 Elsevier Inc. All rights reserved.
doi:10.1016/j.ijheatfluidflow.2007.05.004

Reynolds numbers with an increase in the integral length scale of the FST. They also found that if low-frequency modes diffuse into the boundary layer the streaks are induced by streamwise vorticity through the linear lift-up effect and this process most likely occurs near the leading edge. A non-linear process is needed to generate the streaks if the disturbances are located above the boundary layer. Following Jacobs and Durbin (1998), Zaki and Durbin (2005) demonstrated that certain modes in the freestream are more likely to cause the flow to transition. In that paper they derived a coupling coefficient that characterised the interaction between the continuous spectrum of the Orr-Sommerfeld modes and the boundary layer, this coefficient details the propensity of certain modes in the freestream to penetrate the underlying boundary layer. They showed that with two weakly penetrating freestream modes at the inlet the boundary layer was little perturbed. With two strongly penetrating modes in the freestream, Klebanoff modes were produced but the boundary layer did not transition. With the combination of one weak and one strong penetrating freestream mode the complete transition process was simulated. However, to date, few of these numerically based concepts on the origins of transition have been verified experimentally.

Experimental evidence of the importance of negative fluctuation velocities was demonstrated in the work of Blair (1992), Chong and Zhong (2005) and Hernon et al. (2006). Blair (1992) demonstrated the importance of negative fluctuation velocities with the observation of "negative spike" formations at $y/\delta \approx 0.6$, prior to near-wall turbulent spot formation which contained positive fluctuations when compared to the mean laminar flow. Close to transition onset the negative spikes were shown to develop high-frequency components. Chong and Zhong (2005) illustrated the ensemble-averaged time history of a turbulent spot which was artificially generated by injecting puffs of air through a small orifice in the test surface. In this study structures with negative fluctuation velocity were measured in the upper portion of the boundary layer before positive fluctuations were measured in the near-wall region. Outer edge disturbances of the same form were also discussed by Kendall (1998) and Wundrow and Goldstein (2001). Hernon et al. (2006) used wavelet analysis to investigate the scales and energy content of naturally occurring turbulent structures from the near-wall to freestream regions. The measurements were obtained at approximately 0.1% intermittency, indicating that the flow was very close to the point where the flow first starts breaking down into turbulent motion. It was demonstrated how the internal structure of the turbulent spots change from ones with positive fluctuation velocity near the wall to ones with negative fluctuation velocity near the boundary layer edge when compared to the mean laminar flow. The turbulent structures had a much higher frequency content than the surrounding flow structures and it was also demonstrated that at this very low intermittency there were many more high-frequency turbulent events near the boundary layer edge then there were near the wall.

Westin et al. (1998) examined the receptivity of artificially generated disturbances which were induced upstream of a flat plate. The disturbance generated longitudinal structures of high and low streamwise velocity (previously referred to as streaks). In their experiment the disturbance energy of the longitudinal structures decayed, whereas in experiments under FST the structures grew in magnitude linearly with the displacement thickness (δ_1), thus pointing out the importance of continuous forcing from the FST. The ensemble-average representation of the turbulent structures in Westin et al. (1998) was similar to Chong and Zhong (2005) where negative structures arrive near the boundary layer edge before near-wall positive fluctuations. It is interesting to note that, whether or not the turbulent structures are artificially generated by injecting air from the wall into the boundary layer, or by inducing some upstream deterministic disturbance into the boundary layer, or whether the spots occur naturally, they all have similar flow features. This demonstrates that the disturbances introduced into the flow essentially become receptivity sites for the small scale FST to act on the large scale low-speed streaks.

The connection between disturbances with negative fluctuation velocity in the upper portion of the boundary layer and the development of near-wall turbulent spots has not been determined experimentally. In direct response to this, the current investigation utilises a zero pressure gradient flow in order to gain further insight into the bypass transition process. The measurements are obtained at 4.2% turbulence intensity at the leading edge of the plate. It is the goal of the current investigation to give experimental evidence to corroborate the DNS transition scenario.

2. Experimental facility and measurement techniques

2.1. Experimental facility

All measurements were obtained in a non-return wind tunnel with continuous airflow supplied by a centrifugal fan. Maximum velocities in excess of 100 m/s can be achieved. The settling chamber consists of honeycomb and wire gauze grids which enable the reduction of flow disturbances generated by the fan. Using hotwire anemometry, low-pass filtered at 3.8 KHz, the background turbulence intensity in the working section of the tunnel was measured at 0.2%. The test section dimensions are 1 m in length by 0.3 m width and height.

Table 1 gives the turbulence grid dimensions and the associated range in FST intensities and scales. The turbulence grid was placed at the test section inlet (Fig. 1). The grid was designed and qualified according to the criteria of Roach (1987). The plate leading edge was always placed at least 10 mesh lengths downstream of the grid (see ΔL in Fig. 1) and the isotropy of the freestream turbulence was validated against the von Karman one-dimensional isotro-

Table 1
Geometric description of the turbulence grid and range of turbulence characteristics available, where λ and Λ are the dissipation and integral length scales, respectively. PP relates to the structure of the turbulence grid, where PP refers to perforated plate

Parameter	PP grid
Grid bar width, d (mm)	2.6
Mesh length, M (mm)	25.2
%Grid solidity	20
$\%Tu_{min}$	2
$\%Tu_{max}$	4.3
λ_{min} (mm)	1.5
λ_{max} (mm)	2
Λ_{min} (mm)	5
Λ_{max} (mm)	15

Fig. 1. Illustration of experimental set-up (not to scale).

pic approximation given by Hinze (1975) with excellent agreement (Fig. 2). The turbulence decay rate for the grid compares favourably to the power law relation of Roach (1987) where the percentage turbulence intensity decays to the power of $-5/7$. In the current investigation the leading edge of the plate is placed at 252 mm downstream of the grid which corresponds to 10 mesh lengths giving $\%Tu = 4.2$ for the current test conditions.

The test surface is a flat plate manufactured from 10 mm thick aluminium approximately 1 m long by 0.295 m wide and is placed in the centre of the test section. The leading edge is semi-cylindrical and 1 mm in radius. See Fig. 1 for the experimental arrangement. The flow over the flat plate was qualified as two-dimensional over all measurement planes. The design of the trailing edge flap was shown to anchor the stagnation streamline on the upper test surface thus allowing for zero-pressure gradient to be established facilitating excellent comparison against Blasius theory. The effectiveness of the leading edge design is obvious when considering that the bulk pressure distribution along the length of the plate varies no more than $\pm 1\%$ except for the most upstream static pressure point, located 30 mm downstream of the leading edge, where a 5% drop in dynamic pressure was measured. Further details on the design, manufacture and characterisation of the turbulence grids and the flat plate can be found in Walsh et al. (2005).

2.2. Measurement techniques

Mean and fluctuating velocities were measured using an A.A. Lab Systems AN-1005 constant temperature anemometer. The hotwire and hotfilm probes were operated at overheat temperatures of 250 °C and 110 °C, respectively. All measurements were recorded over 10 s periods

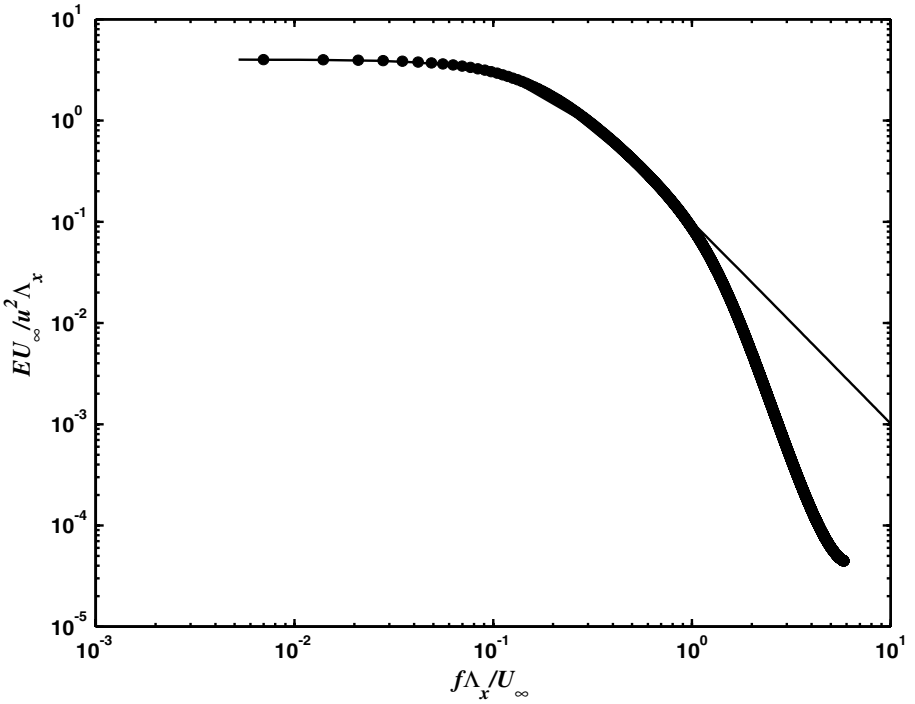

Fig. 2. The freestream energy spectrum compared to the von Karman one-dimensional isotropic approximation (Hinze, 1975). $Re_\theta = 181$ and $\%Tu = 4.2$, where E, U_∞, u, Λ_x and f are the energy spectral density, the freestream velocity, the streamwise fluctuating velocity, the streamwise integral length scale and the frequency, respectively.

at a sampling frequency of 10 KHz and were low-pass filtered at 3.8 KHz to eliminate any noise components at higher frequencies. During any boundary layer traverse the temperature in the test section was maintained constant to within ±0.1 °C. Variation in fluid temperature was compensated for by using the technique of Kavence and Oka (1973). The hotwire calibration was obtained using King's Law between test velocities of 0.4–20 m/s.

In the current investigation transition onset was determined to occur with the observation of approximately one turbulent spot in every 10 s. Using the method of Ubaldi et al. (1996) the onset of transition was detected using a hotfilm sensor (Dantec 55R47) whereby a turbulent spot was determined due to increased heat transfer from the sensor. The dual slope method of Kuan and Wang (1990) was implemented and the near-wall intermittency (γ) was determined to be approximately 0.1%, see Hernon et al. (2006). Using this technique it was found that the Reynolds number at which transition begins compared to within 10% of both the well established correlation of Mayle (1991) and the recent correlation of Fransson et al. (2005). The transition onset Reynolds number in this investigation is $Re_\theta = 181$ and the freestream velocity (U_∞) and boundary layer thickness (δ) at this condition are 3 m/s and 7 mm, respectively. The reason for defining the onset of transition in this way was to ensure very low intermittency levels which indicate that the measurements are at, or very near, the real location of near-wall breakdown thereby giving increased insight into the flow features leading to breakdown.

3. Results and discussion

3.1. Initial flow characteristics

A notable feature of boundary layer flow is the marked change in the sign of the fluctuation velocity (defined as the difference between the instantaneous velocity and the mean velocity) as the boundary layer is traversed from the wall to the freestream. Fig. 3a illustrates the change in flow structure where it is clear that the main structures in the near-wall region have positive fluctuation velocity compared to the structures at the boundary layer edge region with negative fluctuation velocity. The scale of the near-wall structure in Fig. 3b is approximately 16δ. The scale of the negative structure near the boundary layer edge is approximately 3δ. Similar variations in flow characteristics were discussed in Blair (1992) where he termed structures near the boundary layer edge region with negative fluctuation velocity "negative spikes". One such negative spike structure is seen in Fig. 3c.

Fig. 4 illustrates the change in the energy containing scales as the flow is traversed from the near-wall region to the boundary layer edge. The shear sheltering phenomenon can be visualised when examining Figs. 3 and 4 where it is obvious that the boundary layer blocks the high-frequency disturbances from the freestream entering into the boundary layer but permits the lower frequencies to penetrate. This is most obvious when examining Fig. 4 where at the higher frequencies the spectra at $y/\delta \approx 1$ (near the boundary layer edge region) and at $y/\delta \approx 2.8$ (in the free-

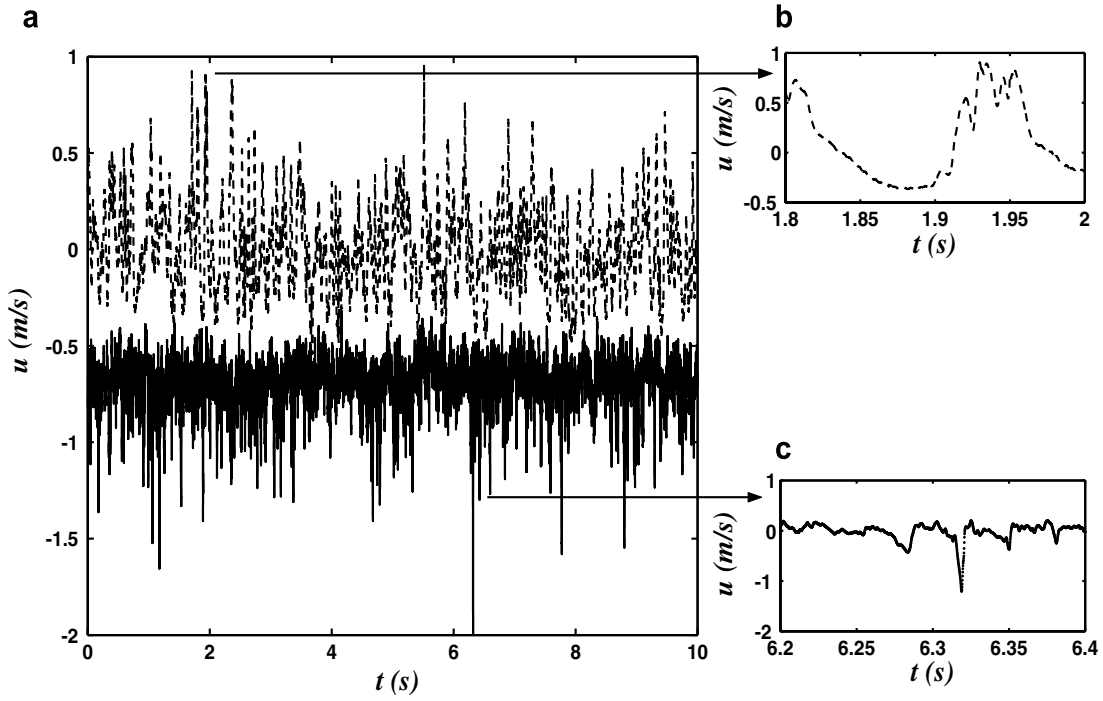

Fig. 3. Illustration of the change in structure of the flow from the near-wall to the boundary layer edge region. (a) Fluctuation velocity traces in the near-wall region, $y/\delta \approx 0.17$, and the boundary layer edge region, $y/\delta \approx 0.9$. The near-wall trace is signified by a dashed line for contrast and the solid line has been shifted for visual representation. (b) Typical flow structure in the near-wall region with positive fluctuation velocity. (c) Typical flow structure in the boundary layer edge region with negative fluctuation velocity. The test conditions are $Re_\theta = 181$, %Tu = 4.2 and $U_\infty = 3$ m/s.

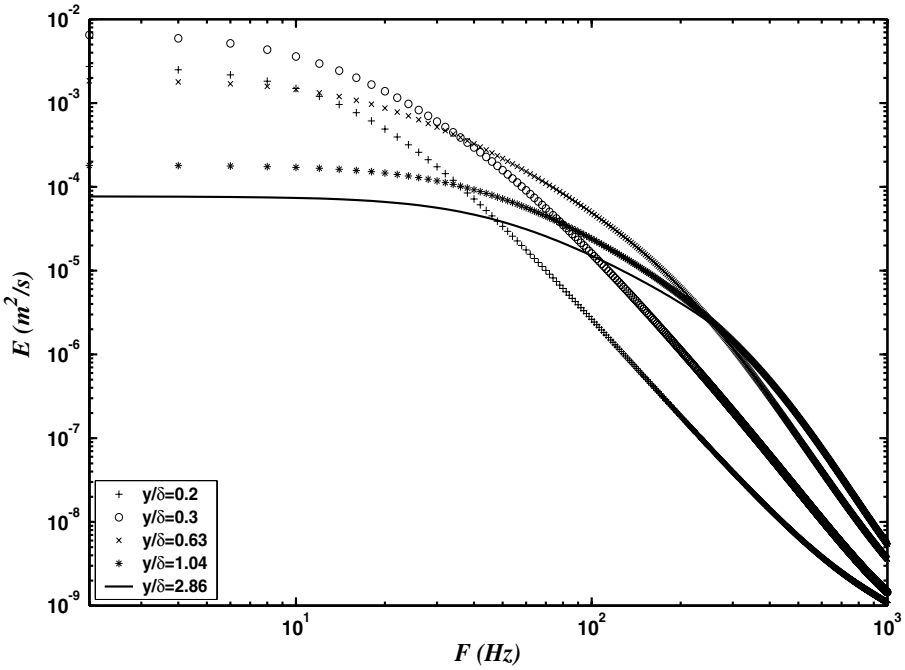

Fig. 4. Energy spectra of the streamwise fluctuating velocity component at transition onset ($Re_\theta = 181$) throughout the boundary layer thickness at %Tu = 4.2.

stream region) are identical; however, at the lower frequencies, the flow near the boundary layer edge region has higher energy content than the freestream. Because the freestream flow does not contain these large scale structures this indicates that such structures must originate from within the boundary layer. This aspect of the flow is qualitatively similar to the DNS transition scenario which demonstrated that low-speed streaks (negative jets) are lifted up towards the boundary layer edge region whereafter they are acted on by the small scale disturbances in the freestream to cause the breakdown to turbulence.

Fig. 5 illustrates the so-called Klebanoff mode disturbance profiles which are the time-averaged representation of the streaky structures in the flow. The profiles are scaled

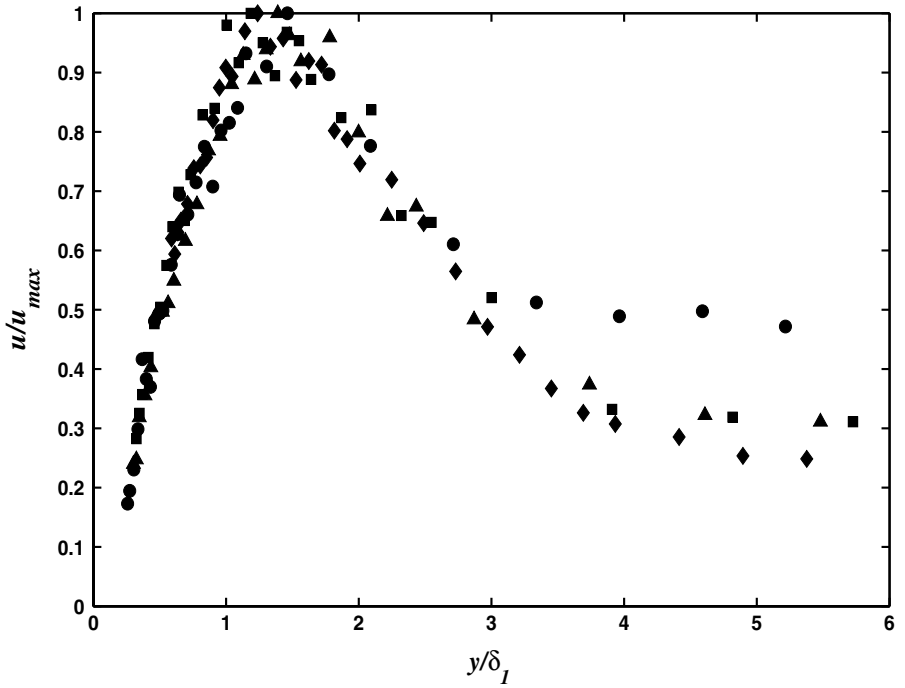

Fig. 5. Illustration of the so-called Klebanoff mode disturbance profiles. ●, $Re_\theta = 76$; ▲, $Re_\theta = 107$; ■, $Re_\theta = 115$; ♦, $Re_\theta = 181$. All measurements at %Tu = 4.2.

with $u_{rms}/u_{rms,max}$, where $u_{rms,max}$ is the peak rms disturbance at each Re_θ. The peak disturbances are observed at $y/\delta_1 \approx 1.4$ ($y/\delta \approx 0.5$) and at transition onset $u_{rms,max}$ is approximately 10% of the freestream velocity, similar to Matsubara and Alfredsson (2001). These profiles resemble closely the theoretical profiles of Andersson et al. (1999) and Luchini (2000) except near the boundary layer edge and freestream regions where the theories fail to predict the turbulent activity. This time-averaged representation of the disturbances in the boundary layer due to the streaky structures is commonplace; however, little information is gained on what type of flow structures may lead to transition as the physically different flow characteristics of the low- and high-speed streaks are masked by the averaging process.

3.2. Instantaneous velocity profiles

Fig. 6 demonstrates the wall-normal distributions of the maximum positive and negative of the streamwise fluctuation velocity in terms of a disturbance magnitude which is defined here as $\%Tu_L = \max|u_{positive/negative}|/U_\infty \times 100$. Here it should be noted that the maximum positive and negative streamwise disturbances are assumed to be due to the passing of high and low-speed streaks over the hot-wire sensor in the laminar flow. From Fig. 6a, which is well upstream of transition onset, it can be seen that the peak positive and negative disturbances, which are associated with the low and high-speed streaks, are approximately equal with $\%Tu_L \approx 20$ at $y/\delta \approx 0.5$. In stark contrast to this, the time-averaged distribution has significantly lower $\%Tu_L$, with $\%Tu_L \approx 6$ at $y/\delta \approx 0.5$. This is an important result as it is a reasonable argument that turbulent spots emerge in the regions of the flow where the largest fluctuations are present, such fluctuations are hidden by the time-averaging analysis in both position and magnitude. Fig. 6b illustrates an interesting change in the flow structure as transition onset is approached. The disturbances associated with the low-speed streaks (or alternatively termed negative jets in DNS terminology) have grown in magnitude above the disturbance level associated with the high-speed streaks (or positive jets). At this point the peak disturbance associated with the low-speed streaks is approximately 30%, according to Andersson et al. (1999) a value sufficient enough to cause secondary instabilities to develop on the streaks and hence the breakdown to turbulence may ensue. The disturbance magnitude of the low-speed streaks is greater than those associated with the high-speed streaks. It is also interesting to note the shift in the relative positioning between the peak locations, where the peak of the low-speed disturbances moved towards the boundary layer edge and the peak of the high-speed disturbances moved towards the wall. Once again the instantaneous profiles have considerably higher disturbance magnitude compared to the time-averaged distributions. Fig. 6c is at a similar Re_θ to Fig. 6b and it is clear that these results are consistent over similar Re_θ thus giving confidence to the 10 s sampling time and further supports the trends in the results. Fig. 6d

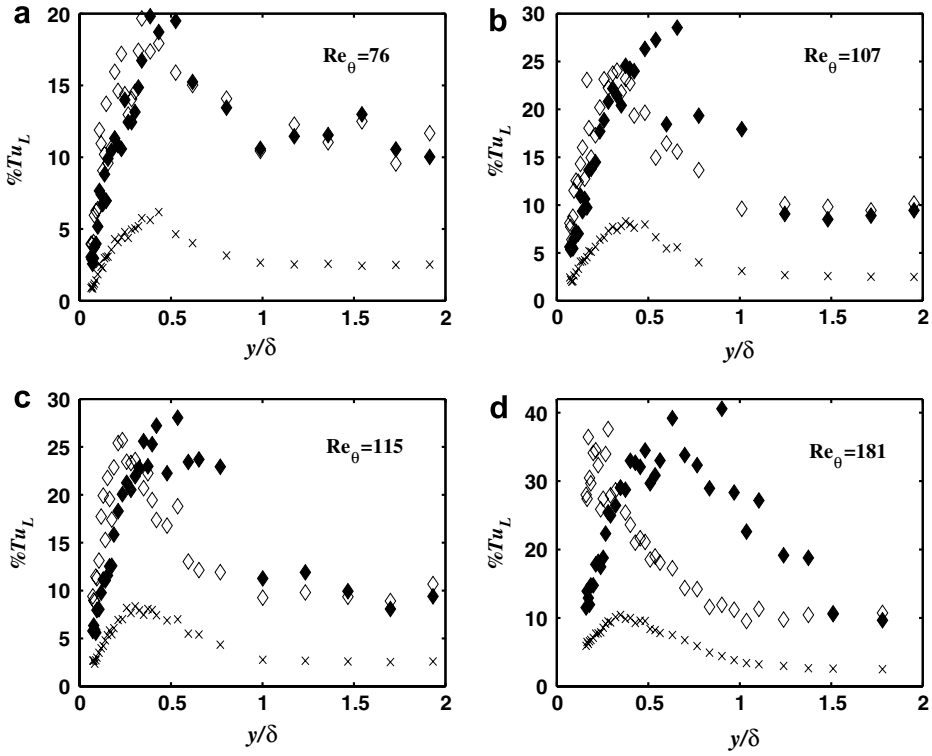

Fig. 6. Maximum positive and negative fluctuation velocities presented in terms of a local disturbance magnitude ($\%Tu_L$) at $\%Tu = 4.2$. (a) $Re_\theta = 76$, (b) $Re_\theta = 107$, (c) $Re_\theta = 115$ and (d) $Re_\theta = 181$ (transition onset). ♦, maximum negative value; ◇, maximum positive value; ×, rms value.

is at transition onset and the peak positive disturbance is again closer to the wall at $y/\delta \approx 0.3$ and the peak negative disturbance has moved closer to the boundary layer edge, $y/\delta \approx 0.9$.

As discussed previously, in relation to Fig. 5, at transition onset the peak time-averaged disturbance has increased in magnitude to approximately 10%Tu_L, which is consistent with previously published time-averaged disturbances at transition onset (Roach and Brierley, 2000; Matsubara and Alfredsson, 2001). This value is once again far below the peak instantaneous values. The shift in the peak positive and negative locations towards the wall and the boundary layer edge regions, respectively, was also demonstrated in the DNS of Brandt et al. (2004) (cf. figure 7) and qualitatively similar to the results presented by Jacobs and Durbin (2001) (cf. figure 14).

The results presented in Fig. 6 illustrate how maximum positive and negative distributions of the streamwise fluctuation velocity give increased insight into the transition process compared to time-averaged results. The fact that the location of the peak negative disturbance (which had greater disturbance magnitude than the positive) shifts toward the boundary layer edge and the peak positive disturbance shifts towards the wall as the point of transition onset is approached gives experimental support to recent DNS results.

3.3. Normalised fluctuation velocity and skewness profiles

Fig. 7a illustrates the maximum positive and negative fluctuation velocity distributions when scaled as u/u_{max}, where u is the maximum instantaneous disturbance on each of the low- and high-speed streaks and u_{max} is the absolute maximum instantaneous disturbance measured on any of the streaks within the boundary layer at each Re_θ. Therefore, when scaled in this way, the profiles represent the signature of the low- and high-speed streaks within the boundary layer and are presented in this way as a comparison to the time-averaged representations which are termed Klebanoff modes (Fig. 5). The maximum positive values demonstrate a good degree of similarity, considering the stochastic and low-intermittent nature of the flow, where the peak locations are in general at $y/\delta \approx 0.3$. The maximum negative values also demonstrate similarity over the range of Reynolds numbers considered, the peak negative values are located in the range $y/\delta \approx 0.5 - 0.9$ (although on average the peak location is at $y/\delta \approx 0.6$). Fig. 7b illustrates the skewness of the fluctuation velocities at the same conditions as Fig. 7a. The skewness is a measure of the lack of statistical symmetry in the signal and is therefore also a measure of the length of the tail on the probability distribution curve. Well upstream of transition onset, $Re_\theta = 76$ in Fig. 7b, the maximum skewness is positive and is located at $y/\delta \approx 0.1$. At this Reynolds number the skewness is zero beyond the boundary layer edge and into the freestream. Moving closer to the location of transition onset (see profiles in Fig. 7b at Re_θ of 107, 115 and 181) the maximum skewness becomes negative. The location of peak negative skewness at these Reynolds numbers is $y/\delta \approx 0.75$. Over this range of Reynolds numbers the skewness profiles collapse up to the location of peak skewness. After the point of peak skewness the profiles deviate considerably depending on their proximity to the location of transition onset, Fig. 7b. As the flow approaches transition onset the skewness remains negative beyond $y/\delta > 1$. These results are in qualitative agreement with the DNS of Zaki and Durbin (2005) (cf. figure 23) where the low-speed streaks lifted past the boundary layer edge. At this stage in the DNS results the lifted low-speed streaks were acted on by the small scale FST which caused a form of Kelvin–Helmoltz instability to develop at the boundary layer edge region and beyond. This plot illustrates the change in flow structure as the flow approaches transition onset; where the internal structure of the flow changes from one with predominantly positive fluctuations well upstream of transition onset to negative fluctuations as transition onset is approached.

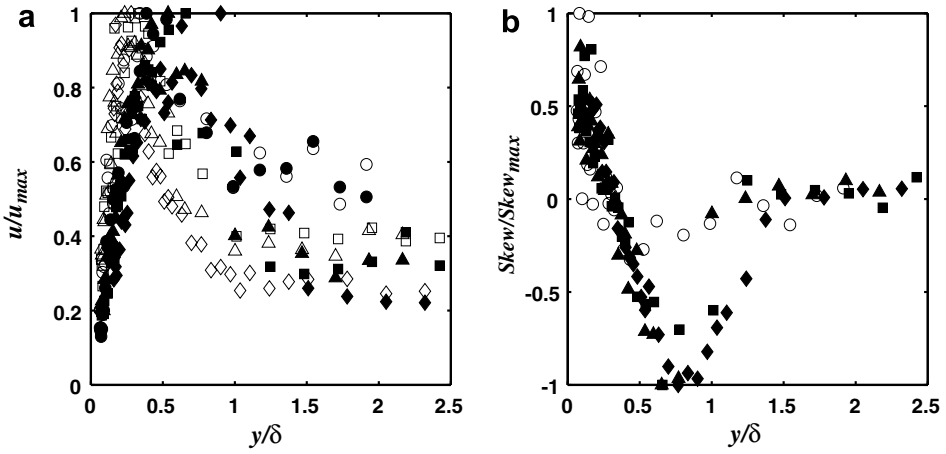

Fig. 7. (a) Wall-normal disturbance profiles of the low and high-speed streaks. (b) Skewness distribution for same conditions in (a). ○, $Re_\theta = 76$; ▲, $Re_\theta = 107$; □, $Re_\theta = 115$; ♦, $Re_\theta = 181$. In (a) open symbols are maximum positive values and closed symbols are maximum negative values. In (b) the open symbols signify the only profile with positive maximum skew. All measurements are at %Tu = 4.2.

The results presented in this investigation demonstrate the importance of negative fluctuation velocities in the transition process and are also the first of an experimental nature at high turbulence intensity to support the transition scenario put forward by DNS. The DNS transition scenario can be summarised as follows: the low-speed streaks (termed negative jets in DNS) lift up towards the boundary layer edge region, due to the motion of vortical structures in the freestream, and are acted on by the small scale disturbances from the freestream. At this point the flow breaks down into patches of turbulence which propagate towards the wall. Although the current results support the transition onset scenario elucidated by DNS, the interaction between the low-frequency lifted low-speed streaks and the high-frequency freestream disturbances is not directly evident in the current findings and more detailed experimental work is needed in this regard.

4. Conclusions

An experimental investigation on a zero pressure gradient flow with elevated freestream turbulence was presented. It was demonstrated how distributions of the maximum positive and negative of the streamwise fluctuating velocity component give increased physical insight into the precursors to turbulent spot production. The importance of instantaneous values over time-averaged results was also demonstrated where the commonplace time-average representation of the Klebanoff mode profiles was shown to mask the very different physical attributes of the low and high-speed streaks. As transition onset is approached the peak negative fluctuation velocity increases in magnitude beyond the positive and its location shifts toward the boundary layer edge. Because the disturbance magnitude is greater on the low-speed streaks this implies that these structures will most probably develop secondary instabilities and breakdown into turbulent motion near the boundary layer edge. The skewness distributions demonstrated the change in flow characteristics as the point of transition onset was approached and represents a potential means of examining the boundary layer in a time-averaged sense while still retaining the important information regarding the receptivity and breakdown process. Well upstream of transition onset the maximum skew had a positive value. As the flow field evolved closer to the point of transition onset the maximum skew changed sign to a negative value. At transition onset the skewness was negative beyond the boundary layer edge, indicating that the low-speed streaks are lifted up past the boundary layer edge and into the freestream whereby they may be acted on by small scale FST to cause the flow to breakdown into turbulent motion, as shown in the DNS results. Both the maximum instantaneous and skewness distributions illustrate how important the negative fluctuation velocities become as the flow evolved towards transition onset. This work represents the first of an experimental nature to support the DNS transition scenario and gives some unique insights into pre-transitional flow and the precursors to turbulent spot formation.

References

Andersson, P., Breggren, M., Henningson, D., 1999. Optimal disturbances and bypass transition in boundary layers. Phys. Fluids 11, 134–150.

Blair, M., 1992. Boundary-layer transition in accelerating flows with intense freestream turbulence: part 1-disturbances upstream of transition onset. J. Turbomach. 114, 313–321.

Brandt, L., Schlatter, P., Henningson, D., 2004. Transition in boundary layers subject to freestream turbulence. J. Fluid Mech. 517, 167–198.

Chong, T., Zhong, S., 2005. On the three-dimensional structure of turbulent spots. J. Turbomach. 127, 545–551.

Fransson, J., Matsubara, M., Alfredsson, P., 2005. Transition induced by free-stream turbulence. J. Fluid Mech. 527, 1–25.

Hernon, D., Walsh, E., McEligot, D., 2006. An investigation using wavelet analysis into velocity perturbations under the influence of elevated freestream turbulence at transition onset. In: ASME Turbo Expo Paper No. GT2006-90987, Barcelona, Spain.

Hinze, J.O., 1975. Turbulence. McGraw-Hill.

Jacobs, R., Durbin, P., 1998. Shear sheltering and the continuous spectrum of the orrsommerfeld equation. Phys. Fluids 10, 2006–2011.

Jacobs, R., Durbin, P., 2001. Simulations of bypass transition. J. Fluid Mech. 428, 185–212.

Kendall, J., 1998. Experiments on boundary-layer receptivity to freestream turbulence. AIAA Paper 98-0530.

Kavence, G., Oka, S., 1973. Correcting hot-wire readings for influence of fluid temperature variations. DISA Information 15, 21–24.

Kuan, C., Wang, T., 1990. Investigation of intermittent behavior of transitional boundary layer using conditional averaging technique. Exp. Therm. Fluid Sci. 3, 157–170.

Luchini, P., 2000. Reynolds-number independent instability of the boundary layer over a flat surface: part 2. optimal perturbations. J. Fluid Mech. 404, 289–309.

Mayle, R., 1991. The role of laminar-turbulent transition in gas turbine engines. J. Turbomach. 113, 509–537.

Matsubara, M., Alfredsson, P., 2001. Disturbance growth in boundary layers subjected to freestream turbulence. J. Fluid Mech. 430, 149–168.

Roach, P., 1987. The generation of nearly isotropic turbulence by means of grids. J. Heat Fluid Flow 8, 82–92.

Roach, P.E., Brierley, D.H., 2000. Bypass transition modelling: a new method which accounts for free-stream turbulence intensity and length scale. ASME Paper No. 2000-GT-0278.

Ubaldi, M., Zunino, P., Campora, U., Ghiglione, A., 1996. Detailed velocity and turbulence measurements of the profile boundary layer in a large scale turbine cascade. ASME 96-GT-4.

Wundrow, D., Goldstein, M., 2001. Effect on a laminar boundary layer of small-amplitude streamwise vorticity in the upstream flow. J. Fluid Mech. 426, 229–262.

Walsh, E.J., Hernon, D.M., Davies, M., McEligot, D., 2005. Preliminary measurements from a new flat plate facility for aerodynamic research. In: Proceedings of the 6th European Turbomachinery Conference, Lille, France.

Westin, K., Bakchinov, A., Kozlov, V., Alfredsson, P., 1998. Experiments on localized disturbances in a flat plate boundary layer. part 1. the receptivity and evolution of a localized free stream disturbance. Eur. J. Mech. B/Fluids 17, 823–846.

Zaki, T., Durbin, P., 2005. Mode interaction and the bypass route to transition. J. Fluid Mech. 531, 85–111.